



INTERNATIONAL JOURNAL OF ENGINEERING SCIENCES & RESEARCH TECHNOLOGY

ION EXCHANGE KINETICS AND EQUILIBRIUM STUDIES OF METAL IONS ONTO A HYBRID CATION EXCHANGER: POLYANILINE–SN(IV)TUNGSTOPHOSPHATE

Arshia Akhtar*, Md. Dilwar Alam Khan, S.A. Nabi

Analytical Research Laboratory, Department of Chemistry, Faculty of Science, Aligarh Muslim
University, Aligarh, India

ABSTRACT

Polyaniline based hybrid cation exchange material Polyaniline–Sn(IV)tungstophosphate (PANI–TWP) has been synthesized by simple sol–gel method and applied for the sorption study of rare earth metal ions on the exchanger. The present investigation deals with the evaluation of feasibility of PANI–TWP toward sorptive removal of rare earth metal ions from aqueous solution. For this various parameters like influence of concentration of metal ions, contact time and temperatures on sorption of ions were investigated using batch method. The sorption process was found to be temperature dependent and increased with the increase in reaction temperature. A comparative kinetic modelling analysis of the sorption data favours the pseudo-second order model and equilibrium adsorption data were best fitted by Langmuir isotherm model for the present system. Apparent activation parameters like activation energy (E_a) and entropy of activation (ΔS^\ddagger) along with self diffusion coefficient (D_i) were also computed using Arrhenius equation. The negative values of $[\Delta S]^\ddagger$ indicate an associative mechanism and there is no significant change in the internal structure of the sorbent during the sorption of counter ions.

KEYWORD: Hybrid cation exchanger, Ion exchange kinetics, Kinetic models, Thermodynamics, Rare earth ions

INTRODUCTION

In the last few years rare earth metal ions have gained much popularity owing to their unique physical and chemical properties [1], versatile chemistry, multitudinous applications like catalyst and other products in industry [2], diagnosis reagents of magnetic resonance imaging (MRI) in medicine, fertilizers in agriculture [3,4] as well as in fluorescent materials. There has been an increasing demand of rare earth elements in whole world for the manufacture of advanced materials. Rare earth elements are also used in making the world's strongest magnets [5]. Neodymium is the third most highly concentrated rare earth element in rare earth ores and used in green technologies. Praseodymium is used in high intensity lighting, mischmetal 'sparking' alloys and exhibits a strong magnetocaloric effect. This property of the element is very important in energy efficient magnetic refrigeration technologies. Gadolinium is used for radiation shielding, phosphor in medical X-ray imaging and a promising element in the development of superconducting materials. The demand for rare earth elements is mainly due to their increased scientific applications in the production of new advanced materials. A minute amount of rare earth element can

enhance the property of metals significantly and it has been regarded as the vitamin of the metals [6].

Nevertheless, they are also having some adverse effects on the environment as well as human health. Reports indicate that the chemicals used in their refining process are responsible for many diseases and destruction of farmland [7]. Health risks are related to their transportation, disposal as well as decommissioning stages [8]. Its exposure can cause negative effects on aquatic and terrestrial organisms including human being.

A large number of techniques are being implemented by the scientist for their separation like liquid-liquid extraction, co-precipitation, ion-exchange [9] and solid phase extraction. Among these the ion exchange process is widely used owing to its superiority in terms of cost, simplicity of design, high removal efficiency, and excellent kinetics. Furthermore, kinetic studies (rate of exchange) do not require a pre treatment step. Also in last few decades ion-exchange has become one of the most important delicate separation process in analytical chemistry with its most spectacular achievement of the separation of rare earth elements in hitherto unknown purity [10].

The kinetic studies envisage the three aspects of ion exchange process, viz. the mechanism of ion exchange, rate determining step and rate laws.

Hence, researchers has the motive to synthesis and investigate various properties of “organic–inorganic” hybrid ion-exchangers which possess better mechanical, chemical, thermal and radiation stabilities, reproducibility and good selectivity for toxic metal ions [11-13] for their useful environmental applications. In most of these fields, information related to the ion exchange kinetics and the mobility of counter ions in the lattice structure is needed.

In the literature a number of papers on synthetic hybrid ion exchange materials with different physical, chemical, and superficial characteristics have been reported which are used as exchange materials for kinetic studies [14-16]. But no systematic investigation of data has been reported because of the different effective diffusion coefficients and different mobility of ions on the ion-exchanger.

In the present endeavour the aim of this work is to synthesize a novel hybrid ion exchanger Polyaniline–Sn(IV)tungstophosphate by sol–gel method and study the kinetic and thermodynamic behaviour of rare earth metal ion exchange on hybrid cation exchanger under diffusion controlled phenomenon. The Nernst–Planck equations [10] with some additional assumptions provide more appropriate values in obtaining the values of the kinetic and thermodynamic parameters precisely. The effect of ionic strength, temperature, time and concentrations on rare earth metal ions exchange are investigated. The removal of heavy metal Pb (II) from waste effluents was also studied to estimate the separation behaviour approaching to a more realistic scenario.

EXPERIMENTAL

Preparation of reagents

All the chemicals and reagents of analytical grade were obtained from E–merck, Aldrich–Chemie, and CDH. For inorganic precipitate, sodium tungstate (0.2 M) and ortho-phosphoric acid (0.2 M) solutions were prepared in DMW and stannic chloride (0.2 M) was prepared in 1 M HCl solution. For the synthesis of organic polymer, ammonium persulfate (0.1 M) and 10% aniline were prepared in 1 M HCl solution. Metal salts used were prepared in triply DMW.

Preparation of Hybrid ion exchanger

The polymerization of aniline was initiated by mixing an equal volume ratio of aniline and ammonium persulfate solutions. The ammonium persulfate solution was added drop by drop in the flask containing aniline solution with continuous stirring for 2 h at a temperature of $8\pm 2^\circ\text{C}$ and the resultant polymer gel was kept for 24 h at the same temperature. The inorganic precipitate of Sn(IV)tungstophosphate was prepared at room temperature by adding a mixture of ortho-phosphoric acid and sodium tungstate to the solution of stannic chloride. A white colour precipitate was formed when the pH of the mixture was adjusted to 0.75 by adding ammonia solution with continuous stirring. Hybrid ion-exchange material was prepared using the sol–gel method in which an equal volume of polyaniline gel and inorganic precipitates of Sn(IV)tungstophosphate was mixed thoroughly with constant stirring at room temperature. The resultant greenish-black slurries were kept for 24 h at room temperature for digestion. The supernatant liquid was then decanted off, filtered and washed thoroughly with DMW to remove excess acid. The dried product was converted into H^+ form by keeping it in an excess of 1M HNO_3 solution for 24 h. The excess acid was removed after several washings with DMW and finally the material was dried in an oven at $50\pm 2^\circ\text{C}$. The desired particles of mean radii (r_0) $\sim 125\ \mu\text{m}$ [50–70 mesh size] were obtained by grinding and sieving the material. In this way a number of samples of Polyaniline–Sn(IV)tungstophosphate (PANI-TWP) were synthesized under variable synthesis conditions as reported in our previous paper [12].

Kinetic Measurements

A digital pH meter (Elico EL 10, India) was used for pH measurements and a temperature variation of $\pm 0.5\ ^\circ\text{C}$ water-bath incubator shaker (MSW22/9550322, Julabo) was used for equilibrium kinetic studies. The metal salts used were of nitrate form. Kinetic and thermodynamic parameters were evaluated by the batch technique method using the ion-exchanger as a sorbent. 300 mg of the sorbent in the H^+ form were taken in different conical flasks containing 30 mL of the different metal ion solutions (Nd^{3+} , Pr^{3+} , Gd^{3+}) and shaken at the desired temperatures for different time intervals for sorption operation. The supernatant liquid was removed and the metal ion concentration was determined by EDTA titration [17-18]. Every set was repeated four-times and the mean values were taken for calculation. The amount of metal ions sorbed per unit sorbent any time, q_t (mg g^{-1}) and the sorption capacity were calculated using the relations

$$q_t = (C_o - C_t) \times \frac{V}{m} \quad (1)$$

$$P = \left(\frac{C_o - C_t}{C_o} \right) \times 100 \quad (2)$$

Where C_o is the initial concentration and C_t is concentration at time t of metal ions in solution, V is the volume of solution and m is weight of the material.

RESULTS AND DISCUSSION

The hybrid cation sorbent PANI-TWP possesses fairly high ion-exchange capacity (1.101 meq g^{-1} for Na^+ ion) with better chemical and thermal stability. For practical viability of the sorbent it is necessary to understand the exchange mechanism, kinetics, thermodynamics, ion chemistry and economics. The electrically charged sites of sorbent are the manifestation of active ionic groups. At these sites, oppositely charged ions are attracted or may be replaced by other ions depending on their respective concentrations and affinities for the sites. Favourability of ions and the number of active sites available for the sorption is resolved by the sorbent effectiveness. When sorbent comes into contact with liquid phase, number of molecules in solution phase decreases due to sorption, with maximum sorption of metal ions initially until equilibrium is reached. During this process some molecules strike and get trapped on the surface of sorbent. The number of molecules sorbed depends on the velocity with which they reach the surface sites of the sorbent and on the rate of binding to the surface.

Effect of concentration and contact time

The effect of metal ion concentrations (0.003–0.018 M) on their uptake by sorbent at room temperature ($25 \pm 2^\circ C$) is shown in Figure 1. It is evident from the figure that with the increase in concentration of metal ions the sorption capacity of metal ions increases from 47–192 mg g^{-1} . Also it indicates that the sorption of metal ions occurs in two distinct steps, with a relatively sharp increase for each concentration at initial stage and then gradually increases to reach equilibrium. A further increase in the contact time has no effect on the sorption of metal ions. Agitation time was fixed for batch experiments to ensure equilibrium process. The equilibrium time was found to be independent of the concentration of metal ions. The discrepancy in the sorption of metal ions is due to the fact that initially all sites on the surface of sorbent were vacant and the concentration of metal ions was relatively high. Thus increase in the uptake of metal ions with time depends on the number of vacant sites present on the surface of sorbent.

Effect of temperature and contact time

The temperature of the solution has pronounced effect on the sorption of metal ions. Generally the rate of sorption increases at higher temperature due to increase in the rate of diffusion of metal ion through the sorbent. Sorption kinetic study reveals that the solute uptake rate and residence time of the sorption reaction is one of the significant characteristic that interprets the sorption capacity of the metal ions. Figure 2 reveals the effect of temperature ($40^\circ C$ – $80^\circ C$) on uptake of metal ions (0.012 M) from aqueous solution by the sorbent. The figure shows that at the same time the sorption capacity of individual metal ions were increased with the increase in temperature indicating the influence of ionic group of sorbent on metal ion sorption equilibrium. The effect of temperature and thermodynamic parameters were calculated using the linear form of Van't Hoff equation [14] to observe the thermodynamic feasibility of the process.

$$\ln K = \left(\frac{\Delta S^\circ}{R} \right) - \left(\frac{\Delta H^\circ}{RT} \right) \quad (3)$$

$$\Delta G^\circ = \Delta H^\circ - T\Delta S^\circ \quad (4)$$

where ΔG° is the standard free energy (KJ mol^{-1}), ΔH° is the standard enthalpy (KJ mol^{-1}), ΔS° is the standard entropy (J $mol^{-1}K^{-1}$), K is the sorption equilibrium constant and T is the sorption temperature (K). The values of ΔH° and ΔS° were calculated from the slopes and the intercepts of the linear plot of $\ln K$ versus $1/T$ (Figure 3). On the basis of these two parameters ΔG° was determined. The ΔG° values were found to be negative at all temperatures, demonstrating the thermodynamic feasibility and spontaneity of the sorption process. The value of ΔH° for rare earth metal ions was found to be positive indicating the reaction is endothermic. The positive value of ΔS° indicates that there is an increase in randomness at the solid-solution interface with some structural changes in the sorbent as well as sorbate (Table 1).

Sorption kinetic model studies

Sorption kinetic models are the area of analytical chemistry related to the rate and speed at which the chemical reaction occurs. There are a number of sorption kinetic models available that evaluate the sorption mechanism of metal ions on the surface of sorbent. Rate of sorption is proportional to the number of active sites occupied and the driving force on the sorbent surface. It is now well accepted that the two parameter sorption models i.e Lagergren pseudo first-order [19] and Ho pseudo second-order [20] are significant tool to explain the sorption mechanism on the sorbent. In addition, the

intraparticle diffusion and homogeneous particle diffusion model are also used to explain the sorption phenomenon. The best fit model was selected on the basis of linear regression correlation coefficients (R^2), which evaluate the forecast values from models.

Lagergren pseudo first-order kinetic model

In a reversible reaction when an equilibrium sorption state of metal ions is established between two phases where external mass transfer reaction takes place from liquid phases to solid phases, Lagergren pseudo first-order rate equation may be linearly expressed as:

$$\log(q_e - q_t) = (\log q_e) - \left(\frac{k_1}{2.303} t\right) \quad (5)$$

Where q_e and q_t (mg g^{-1}) are the amount of metal ion sorbed at equilibrium and at time t respectively. K_1 is the pseudo first order rate constant (min^{-1}). The plots between $\log(q_e - q_t)$ against different temperature t (Figure 4) are used to investigate the appropriateness of pseudo first-order model. K_1 , q_e and correlation coefficient (R^2) were determined from equation (5) at all temperature.

Ho pseudo second-order kinetic model

The pseudo second-order rate model is also applied to understand the kinetics of sorption of metal ions onto sorbent material. The chemisorptions kinetic rate equation is linearly expressed as:

$$\left(\frac{1}{q_e - q_t}\right) = \left(\frac{1}{q_e}\right) + k_2 t \quad (6)$$

Eq. (6) can be rearranged to obtain a linear form as:

$$\left(\frac{t}{q_t}\right) = \left(\frac{1}{k_2 q_e^2}\right) + \left(\frac{t}{q_e}\right) \quad (7)$$

Initial sorption rate 'h' ($\text{mg L}^{-1} \text{min}^{-1}$) is:

$$h = k_2 q_e^2 \quad (8)$$

Then eq. (7) and (8) become:

$$\left(\frac{t}{q_t}\right) = \left(\frac{1}{h}\right) + \left(\frac{t}{q_e}\right) \quad (9)$$

The kinetic linear plot between t/q_t versus t for the sorption of rare earth metal ion at different temperature is shown in Figure 5. The values of q_e , k_2 , h and R^2 were determined from the slope and intercept of the plot. The values of correlation coefficient (R^2) suggest a strong relationship between the parameters and also explain the sorption process of each metal ions follow the pseudo second order kinetic model.

These results indicate the pseudo second-order model better fits for sorption mechanism and overall rate constant of each metal ion appears to be controlled by the chemisorptions process.

A comparative study of the two kinetic models for the sorption process showing the values of rate constants and correlation coefficients (R^2) are presented in Table 2. The value of correlation

coefficient (R^2) recommends a good relationship between parameters and describes the sorption kinetics of each metal ion fits pseudo second-order kinetic model. Also the metal ion sorption ' q_e ' and rate constant ' k_2 ' were increased with the increase of temperature. The value of correlation coefficients (R^2) (>0.91 or nearer to 1) indicates that the pseudo second-order kinetic model better fits for the present system.

Sorption isotherm model

In general, sorption isotherm is an invaluable curve that describes the retention or mobility of substance from aqueous media to solid phase at constant temperature and pH. The sorption equilibrium is established when the sorbent surface is brought into contact with sorbate phase for sufficient time. The sorption data were calculated using three different two-parameter isotherm models.

Langmuir isotherm

The Langmuir isotherm [21] assumes a monolayer sorption for each molecule on the sorbent surface containing a finite number of sorption sites that are equivalent and identical with no lateral interaction and steric hindrance between the adsorbed molecules. There is a uniform strategy of the sorption with no transmigration of metal ion solutions on the plane of surface [22]. It determines the relationship between the amount of metal ion adsorbed on the sorbent surface and the concentration of metal ions remaining in the liquid phase. The linear form of Langmuir isotherm for an equilibrium condition is given by the following equation:

$$\left(\frac{C_e}{q_e}\right) = \left(\frac{1}{Q_0 b}\right) + \left(\frac{1}{Q_0}\right) \cdot C_e \quad (11)$$

where C_e is the equilibrium concentration of metal ions in solution (mg mL^{-1}), q_e is the equilibrium concentration of metal ions on the sorbent surface (mg g^{-1}), b is the equilibrium constant related to the binding energy of the sorption and Q_0 is the monolayer sorption capacity of the sorbent (mg g^{-1}) correlated with the variation of the surface area and porosity of the materials. Higher surface area and pore volume will result in higher sorption capacity. The plots of C_e/q_e versus C_e for the sorption of metal ions onto sorbent surface give a straight line with slope of $1/Q_0$ and intercept $1/Q_0 b$ (Figure 6a). The value of the correlation coefficients (R^2) is found to be 0.996, 0.994 and 0.997 for Pr^{3+} , Nd^{3+} and Gd^{3+} respectively.

Hereby, the essential characteristic of Langmuir isotherm is exhibited by a dimensionless constant called the equilibrium parameter (R_L). The R_L is defined as:

$$R_L = \frac{1}{1 + bC_0} \quad (12)$$

where b is the Langmuir constant and C_0 is the initial concentration of metal ion (mg mL^{-1}). R_L values indicate the type of isotherm and sorption to be either unfavourable ($R_L > 1$), linear ($R_L = 1$), favourable ($0 < R_L < 1$) or irreversible ($R_L = 0$). The R_L values for rare earths on the sorbent surface as obtained from the experimental data were between 0–1 indicating favourable sorption.

3.4.2. Freundlich isotherm

This model is considered for multilayer sorption on heterogeneous surface with uniform energy. Linear form of Freundlich isotherm [23] is given by following equation:

$$\ln q_e = \ln K_f + \left(\frac{1}{n}\right) \ln C_e \quad (13)$$

where K_f and n are Freundlich constants, n is related to the intensity of the sorption which varies with sorbent heterogeneity. K_f (mg g^{-1}) is related to the sorption capacity of the sorbent. Sorption intensity and surface heterogeneity is measure by the slope $1/n$ (range 0–1), becoming more heterogeneous as the value approaches closer to zero. A value below one indicates a normal Langmuir isotherm whereas the value above one is indicative of cooperative sorption [24]. The plot of $\ln q_e$ versus $\ln C_e$ gave a straight line with slope of $1/n$ and intercept K_f (Figure 6b). The values of correlation coefficients (R^2) were found to be 0.994, 0.990 and 0.988 for Pr^{3+} , Nd^{3+} and Gd^{3+} respectively. The Freundlich $1/n$ values are less than 1 indicating a favourable sorption process.

Dubinin–Radushkevich (D–R) isotherm

Another model for the analysis is Dubinin–Radushkevich isotherm with high degree of rectangularity model to calculate the mean free energy of the sorption per molecule of sorbent and further reckoning the sorption behaviour of the sorbent can be expressed by following equation [25]

$$q_e = q_{m,DR} e^{-\beta \varepsilon^2} \quad (14)$$

Taking the logarithm on both side of equation (14) we obtain the following equation:

$$\ln q_e = \ln q_{m,DR} - \beta \varepsilon^2 \quad (15)$$

where $q_{m,DR}$ is the Dubinin–Radushkevich monolayer sorption capacity (mg g^{-1}), β is Dubinin–Radushkevich constant and ε is the Polanyi potential related to the equilibrium concentration as [26]

$$\varepsilon = RT \ln \left(1 + \frac{1}{C_e}\right) \quad (16)$$

The constant β is related to the mean free energy E of sorption per molecule of the sorbent and can be calculated using following relationship:

$$E = \frac{1}{\sqrt{2\beta}} \quad (17)$$

This constant β and sorption capacity $\ln q_{m,DR}$ can be obtained from the linear plot of $\ln q_e$ against ε^2 (Figure 6c). The value of E in the range of 1–8 and 8–16 kJ mol^{-1} forecasts the physical sorption and chemical sorption respectively. The E values obtained in our work are ascribed to the chemisorptions of rare earths by PANI–TWP. The values of correlation coefficients R^2 is found to be lower than Langmuir isotherm. Thus, the D–R model does not fit the data closely.

Figure 6 illustrates all the three isotherm models i.e Langmuir, Freundlich and Dubinin–Radushkevich (D–R) considered for sorption of rare earth metal ions. The corresponding sorption data for rare earth ions on hybrid sorbent are summarized in Table 3. From all the models considered above it can be shown that Langmuire model with $R^2 > 0.9$ best fits the experimental data for the sorption of rare earth metal ions on the PANI–TWP cation sorbent material. The experimentally obtained sorption capacity for Pr^{3+} , Nd^{3+} , Gd^{3+} were found to be 47.91, 47.21, 48.74 mg g^{-1} of sorbent, this agrees well with the capacity determined by Langmuir model. It further confirms the Langmuir fit to the present system.

Diffusion models

Intraparticle diffusion model

Diffusion mechanism of ions can be studied by the intraparticle diffusion model. Mechanism of diffusion is influenced by the transport process. During transport process, the sorbate metal ions transferred from bulk of the solution to the solid surface. The intraparticle diffusion model given by Morris and Weber [27] can be expressed as:

$$q_t = k_{id} t^{1/2} + C_i \quad (19)$$

where k_{id} is intraparticle diffusion rate constant ($\text{mg g}^{-1} \text{min}^{-1/2}$) and C_i is boundary layer diffusion. According to the equation (19) a linear plot a graph between q_t against $t^{1/2}$ shows diffusion controlled phenomenon (Figure 7). Larger the intercept greater is the boundary layer effect [28]. The intraparticle diffusion rate constant k_{id} and boundary layer diffusion C_i were calculated from the slopes and intercepts of linear plots.

Homogeneous particle diffusion model (HPDM)

According to this model, the potential rate–determining step can be explained by two processes (a) interdiffusion of ions within the beads surface called particle diffusion mechanism, or (b) inerdiffusion of ions through the adherent film surrounding by the particle called film diffusion mechanism. Nernst–Plank equation which considered both concentration and electrical gradients of exchanging ions into the flux equation was used to

establish the HPDM equation. If diffusion of ions through the sorbent beads is the slowest step then the rate determining step is particle diffusion controlled. Particle diffusion model can be applied to calculate the diffusion coefficients of the particle using following equation [29].

$$-\ln(1-F^2) = \frac{3D_i\pi^2}{r_0^2} t \quad (20)$$

where D_i is the particle diffusion coefficient, F is the fractional attainment of equilibrium and r_0 is the radius of sorbent. If diffusion of ions from the solution to the sorbent through the adherent film is slowest step then the rate determining step is film diffusion controlled. The film diffusion control may prevail in system with sorbent having higher concentration of fixed ionic groups, low degree of cross linking, small particle size and insufficient agitation. In such case following equation is utilized to calculate the diffusion coefficient as:

$$-\ln(1-F) = \frac{3D_i C_l}{r_0 \delta C_s} t \quad (21)$$

where D_i the diffusion coefficient in the liquid phase, δ is the thickness of the liquid film, C_l and C_s are the concentration of the ion in liquid and solid phases respectively.

Both model equation (20) and (21) were tested for the kinetic rate data of sorbent at different temperature for rare earth metal ions sorption. The graph plot between $-\ln(1-F)$ and $-\ln(1-F^2)$ against contact time is shown in Figure 8. The diffusion coefficient values of both models were calculated from the slope of the straight line and reported along with correlation coefficient (R^2) values in Table 4. In case of the film diffusion model, the straight line does not pass through the origin (graphs omitted) indicating that the film diffusion does not control rate of sorption process. On the other hand, in case of particle diffusion model the straight line passing through the origin indicated that the particle diffusion model controls sorption process at all studied temperatures. The slope values of these plots were used to calculate the effective diffusion coefficients (D_i) using Equation (21). The magnitude of the diffusion coefficient is dependent upon the nature of the sorption process. For physical sorption, the value of the effective diffusion coefficient ranges from 10^{-6} to 10^{-9} m^2/s and for the chemisorptions, the value ranges from 10^{-9} to 10^{-17} m^2/s [30]. Therefore, the most likely nature of the sorption is chemisorption since the values of D_i were in the order 10^{-10} m^2/s , whereas the molecules are strongly bound and mostly localized. Also, based on the values of the correlation coefficient (R^2) the HPDM models were found to best correlate the rate kinetic data of the sorption of rare earth metal ions.

3.6. Apparent activation energy

The Arrhenius activation energy [30] can be calculated from the value of effective diffusion coefficient at different temperature using Arrhenius relation:

$$\ln D_i = \ln D_0 - \left(\frac{E_a}{RT}\right) \quad (22)$$

Where D_0 the pre-exponential constant, E_a is the activation energy of sorption in $KJ mol^{-1}$, R is the gas constant ($8.314 J mol^{-1} K^{-1}$) and T is the absolute temperature (K). The graph plot between $\ln D_i$ versus $1/T$ gives straight line as shown in Figure 9. The apparent activation energies (E_a) for these metal ions were calculated from the slopes of the straight lines. The E_a value of 5–40 $KJ mol^{-1}$ generally signifies the predominance of physisorption process whereas a value of 40–800 $KJ mol^{-1}$ designates an activated chemical sorption [31]. Therefore a low value of E_a in the present case indicates that the studied sorption might be a physisorption process. The value of entropy of activation energy indicates whether or not the reaction follows an associative or dissociative mechanism. The entropy of activation (ΔS^*) was calculated using the following relation [32]

$$D_0 = 2.72d^2 \left(\frac{kT}{h}\right) \cdot \exp\left(\frac{\Delta S^*}{R}\right) \quad (23)$$

where h is the Plank constant, k is the Boltzmann constant; d is the average distance between the active sites on the sorbent surface and assumed to be equal to 5 Å and T is the temperature on the Kelvin scale.

The calculated E_a and ΔS^* values for the present system are presented in Table 5. The negative value of ΔS^* indicates an associative mechanism and there is no significant change in the internal structure of the sorbent during sorption. This recommends that the sorption of ions from solution occurs with partial desolvation of ions at the active sites of the sorbent surface.

CONCLUSION

The approach adopted in this work has proved to be successful and meets the best analytical requirements such as simple design and instrumentation with an easy functioning and a low cost of acquisition and maintenance. A concatenation of kinetics and thermodynamic process involves ions of different mobility and charges which is convenient for understanding the ion-exchange behaviour of rare earth metal ions. The experimental data were interpreted by widely used approaches and models where the ion-exchange kinetics procedure was proved to be a simple, accurate, sensitive, selective, repeatable, and environmentally innocuous method for efficient separation of rare earth metal ions using PANI–TWP cation exchanger as a sorbent. The

correlation coefficient values supports the pseudo second order model and kinetic data were best fitted by Langmuir adsorption isotherm. On the basis of ion-exchange kinetics, entropy and enthalpy of activation, the cation sorbent was found to be suitable for separation of rare earths and for environmental remediation processes.

ACKNOWLEDGEMENT

We are thankful to the Chairman, Department of Chemistry, Aligarh Muslim University, Aligarh for providing research facilities and University Grants Commission (India) for the award of UGC-BSR faculty fellowship to Prof. Syed Ashfaq Nabi.

REFERENCES

- [1] An F, Gao B, Huang X, Zhang Y, Li Y, Xu Y, Chen Z, Gao J (2013) Removal of Fe(II) from Ce(III) and Pr(III) rare earth solution using surface imprinted polymer. *Desalin Water Treat* 51: 5566–5573.
- [2] Chunhua X, Xiaozheng L, Caiping Y (2008) Effect of pH on sorption for RE(III) and sorption behaviors of Sm(III) by D152 resin. *J Rare Earth* 26: 851–856.
- [3] Liang P, Liu Y, Guo L. Determination of trace rare earth elements by inductively coupled plasma atomic emission spectrometry after preconcentration with multiwalled carbon nanotubes. *Spectrochim. Acta. B.*, 2005, 60: 125–129.
- [4] Chunhua X, Zhanwang Z (2010) Evaluation of D113 cation exchange resin for the removal of Eu(III) from aqueous solution. *J Rare Earth* 28: 862–867.
- [5] Horikawa T, Itoh M, Suzuki S, Machida K (2004) Magnetic properties of the Nd-Fe-B sintered magnet powders recovered by Yb metal vapor sorption. *J Magn Magn Mater* 271: 369–380.
- [6] Zhanwang Z, Chunhua X (2011) Adsorption behavior of ytterbium (III) on gel-type weak acid resin. *J Rare Earth* 29: 407–412.
- [7] Rim KT, Koo KH, Park JS (2013) Toxicological evaluations of rare earths and their health impacts to workers: A literature review. *HSWA* 4: 12–26.
- [8] Paul J, Campbell G (2011) Additional review by Region 8 Mining Team Members. Washington, DC: Environmental protection agency (US) Report No.: EPA Document-908R11003.
- [9] Nilchi A, Khanchi A, Atashi H, Bagheri A, Nematollahi L (2006) The application and properties of composite sorbents of inorganic ion exchangers and polyacrylonitrile binding matrix. *J. Hazard. Mater* 137: 1271–1276.
- [10] Helfferich F (1962) *Ion Exchange*, McGraw-Hill, New York.
- [11] Nabi SA, Shalla AH (2009) EDTA–stannic(IV)iodate: preparation, characterization and its analytical applications for metal content determination in real and synthetic samples. *J Porous Mater* 16: 587–597.
- [12] Nabi SA, Akhtar A, Khan MdDA, Khan, MA (2014) Synthesis, characterization and electrical conductivity of Polyaniline–Sn(IV)tungstophosphate hybrid cation exchanger; analytical application for removal of heavy metal ions from wastewater. *Desalination* 340: 73–83.
- [13] Khan MdDA, Akhtar A, Nabi SA (2014) Kinetics and thermodynamics of alkaline earth and heavy metal ion exchange under particle diffusion controlled phenomenon using Polyaniline–Sn(IV)iodophosphate Nanocomposite. *J Chem Eng Data* 59: 2677–2685
- [14] Roy A, Chakraborty S, Kundu SP, Adhikari B, Majumder SB (2012) Adsorption of anionic-azo dye from aqueous solution by Lignocellulose-Biomass jute fiber: equilibrium, kinetics, and thermodynamics study. *Ind Eng Chem Res* 51: 12095–12106.
- [15] Islam A, Ahmad H, Zaidi N, Yadav S (2013) Selective separation of Aluminum from biological and environmental samples using Glyoxal-bis(2-hydroxyanil) functionalized Amberlite XAD-16 Resin: kinetics and equilibrium studies. *Ind Eng Chem Res* 52: 5213–5220.
- [16] Chen L, Lü L, Shao W, Luo F (1961) Kinetics and equilibria of Cd(II) adsorption onto a chemically modified lawn Grass with H[BTMPP]. *J Chem Eng Data* 56: 1059–1068.
- [17] Reilley CN, Schmidt RW, Sadek FS (1959) Chelon approach to analysis (I) survey of theory and application. *S J Chem Edu* 36: 555–564.
- [18] Vogel AI (1961) *A Text-book of quantitative inorganic analysis* longmans, London.
- [19] Lagergren S (1898) Zur theorie der sogenannten adsorption gelöster stoffe, *Kungliga Svenska Vetenskapsakademiens. Handlingar* 24: 1–39.
- [20] Ho YS, Mckay G (1999) Pseudo-second order model for sorption processes. *Process Biochem* 34: 451–465.
- [21] Langmuir I (1918) The adsorption of gases on plane surfaces of glass, mica and platinum. *J Am Chem Soc* 40: 1361–1402.

- [22] Foo KY, Hameed BH (2010) Insights into the modeling of adsorption isotherm systems. *Chem Eng J* 156: 2–10.
- [23] Freundlich HMF (1906) Over the adsorption in solution. *J Phys Chem* 57: 385–470.
- [24] Khan AA, Ahmad R, Khan A, Mondal PK (2013) Preparation of unsaturated polyester Ce(IV) phosphate by plastic waste bottles and its application for removal of Malachite green dye from water samples. *Arab J Chem* 6: 361–368.
- [25] Dubinin MM, Radushkevich LV (1947) The equation of the characteristic curve of the activated charcoal. *Proc Acad Sci USSR, Phys Chem Sect* 55: 331–337.
- [26] Polanyi M (1932) Theories of the adsorption of gases. A general survey and some additional remarks. *Trans Far Soc* 28: 316–333.
- [27] Weber WJ, Morris JC (1963) Kinetics of adsorption on carbon from solution. *J Sanit Eng Div Am Soc Civil Eng* 89: 31–59.
- [28] Achmad A, Kassim J, Suan TK, Amat RC, Seey TL (2012) Equilibrium, kinetic and thermodynamic studies on the adsorption of direct dye onto a novel green adsorbent developed from *Uncaria Gambir* extract. *J Phys Sci* 23: 1–13.
- [29] Boyd GE, Adamson AW, Myers Jr, L S (1947) The exchange adsorption of ions from aqueous solutions by organic zeolite (II) kinetics. *J Am Chem Soc* 69: 2836–2848.
- [30] El-Naggar IM, Zakaria, Ali IM, Khalil M, El-Shahat MF (2012) Kinetic modeling analysis for the removal of cesium ions from aqueous solutions using polyaniline titanotungstate. *Arab J Chem* 5: 109–119.
- [31] Scheckel KG, Sparks DL (2001) Temperature effects on nickel sorption kinetics at mineral-water interface. *Soil Sci Soc Am J* 65: 719–728.
- Laidler KJ (1965) *Chemical kinetics*, second ed. McGraw-Hill, New York.

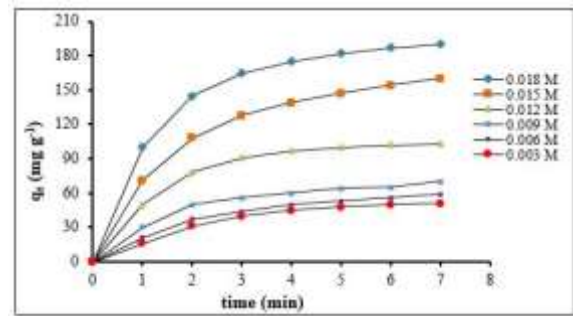
FIGURE CAPTIONS:

Figure 1: Effect of metal ion concentrations and contact time for M(III)–H(I) exchanges at 25±2°C using PANI–TWP cation sorbent.

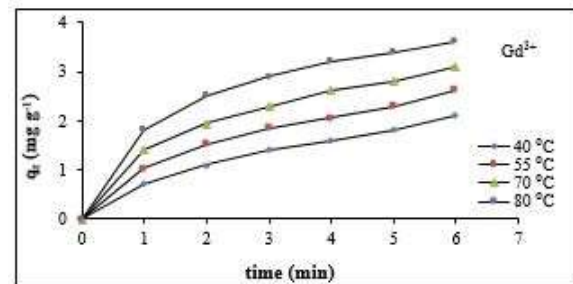
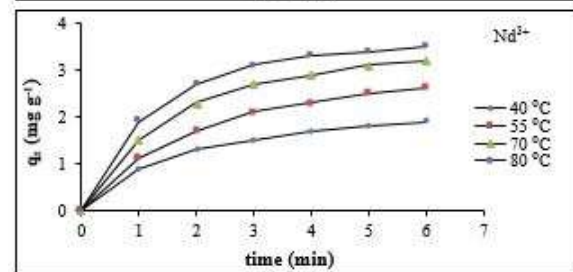
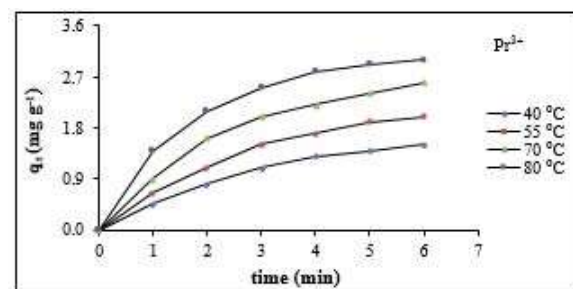


Figure 2: Effect of temperature and contact time on the amount of rare earth ions sorbed on PANI–TWP.

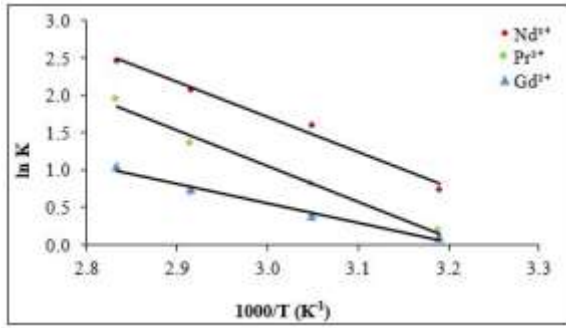


Figure 3: Plots of sorption equilibrium versus temperature ($1/T$) for sorption of rare earth ions on PANI-TWP.

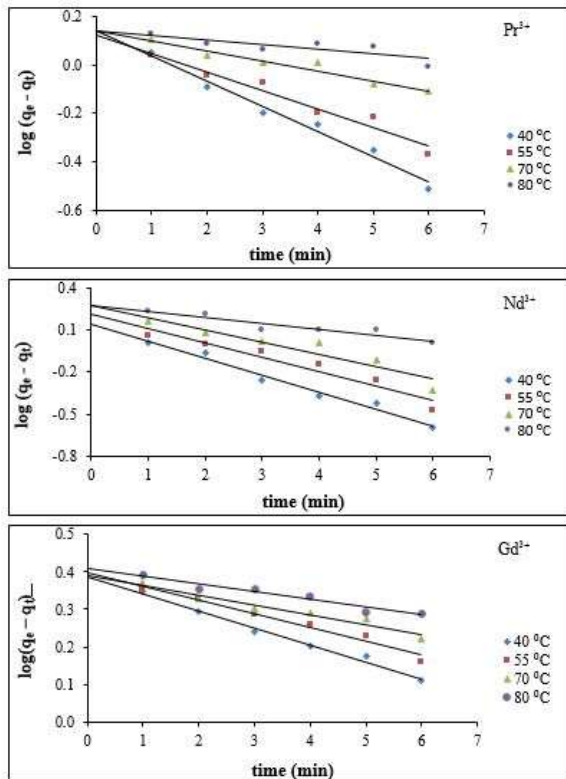


Figure 4: Pseudo first-order kinetic plots for the sorption of rare earth ions on PANI-TWP cation sorbent at different temperatures.

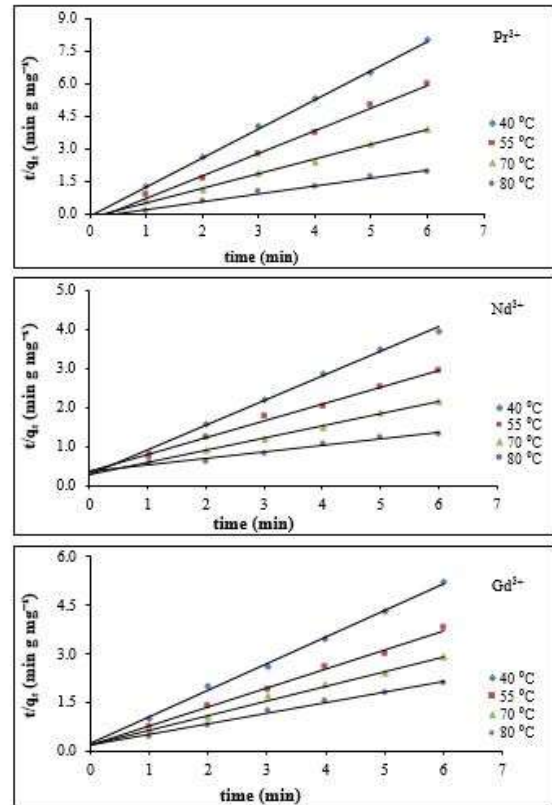


Figure 5: Pseudo second-order kinetic plots for the sorption of rare earth ions on PANI-TWP cation sorbent at different temperature.

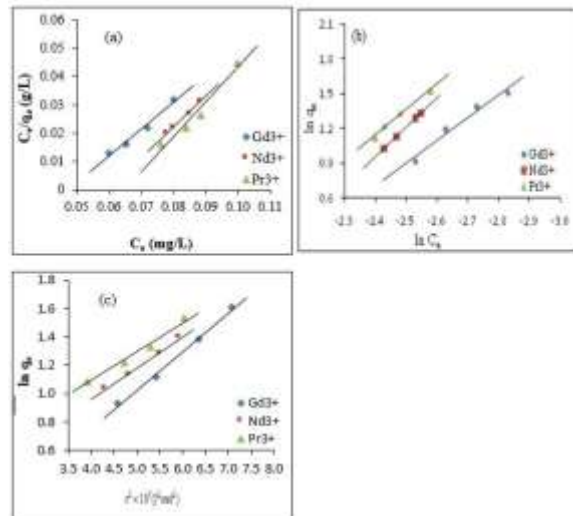


Figure 6: (a) Langmuir (b) Freundlich and (c) Dubinin-Radushkevich (D-R) sorption isotherm of rare earth ions on PANI-TWP cation sorbent.

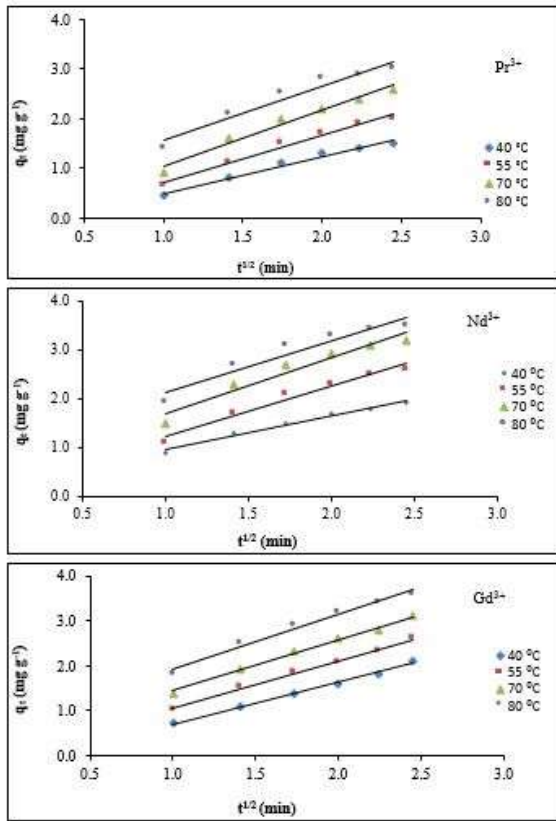


Figure 7: Morris and Weber kinetic plots for the sorption of rare earth ions on PANI-TWP cation sorbent.

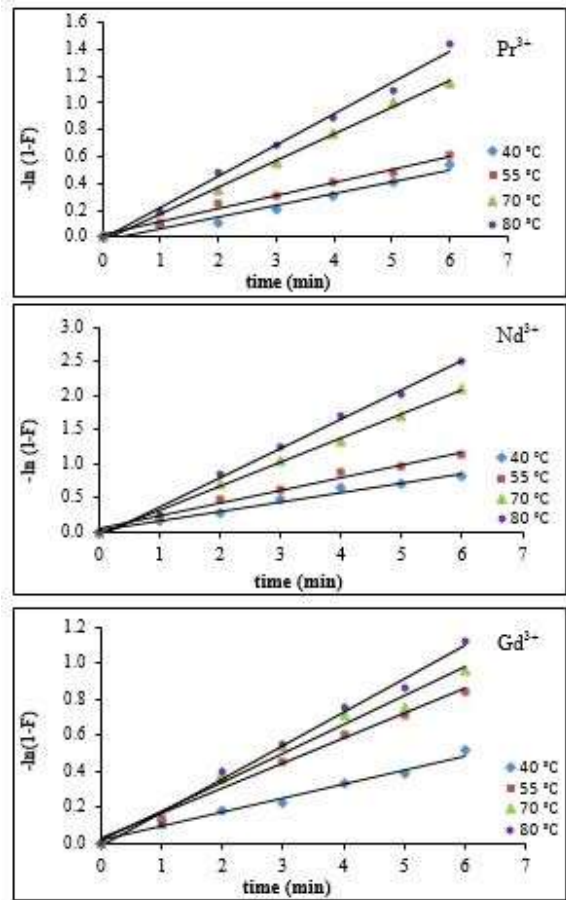


Figure 8: Plots of $-\ln(1-F)$ as a function of time for the diffusion of rare earth ions on PANI-TWP cation sorbent at different temperature.

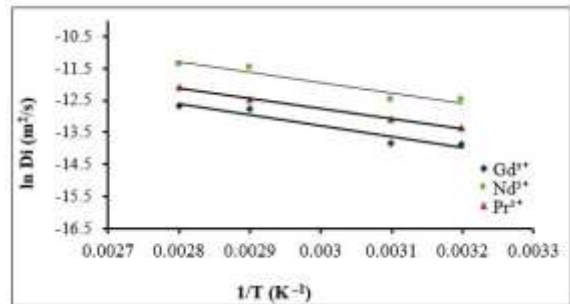


Figure 9: Arrhenius plots for the particle diffusion of rare earth ions on PANI-TWP cation exchanger sorbent.